Exosome derived from bone marrow mesenchymal stem cells pre-treated with curcumin alleviates osteoporosis by promoting osteogenic differentiation via regulating the METTL3/microRNA-320/RUNX2 signaling pathway

Type

Research paper

Keywords

curcumin, osteoporosis, bone marrow stem cells, Exosome, Runx2, METTL3, miRNA-320

Abstract

Introduction
Curcumin (CUR) was reported to stimulate the expression of methyltransferase□like 3 (METTL3), a potential new target for the replacement therapy of osteoporosis. Besides, marrow stem cells (MSC)-derived exosomes (EXO) were proven to improve osteoporosis by promoting the proliferation of osteoblasts. In this study, we aimed to study the effect of CUR and BMSC-derived exosomes in the treatment of osteoporosis.

Material and methods
Microscopy was used to characterize exosomes derived from bone marrow stem cells (BMSCs). MicroCT was carried out to analyze the parameters of bone formation. Western blot was carried out to analyze the expression of surface markers on BMSC-derived exosomes and METTL3/Runt-related transcription factor 2 (RUNX2) proteins under different conditions. Real-time PCR was used to assess the gene expression under different circumstances.

Results
The exosomes derived from CUR-treated BMSCs showed an enhanced therapeutic effect on osteoporosis mice compared with exosomes derived from untreated BMSCs. Mechanistically, the effect of BMSC-derived exosomes on restoring the de-regulated expression of METTL3, miR-320 and RUNX2 was significantly enhanced by CUR treatment upon BMSCs. Besides, CUR treatment upon BMSCs showed an obvious effect on enhancing the stimulatory role of BMSC-derived exosomes in the expression of METTL3, miR-320, RUNX2, BGLAP and LAP in BMSCs. Furthermore, luciferase assay demonstrated that miR-320 was capable of suppressing the expression of RUNX2 through binding to the 3’ UTR of RUNX2.

Conclusions
Our study demonstrated that BMSC-derived exosomes could modulate the METTL3/miRNA-320/RUNX2 axis to attenuate osteoporosis by promoting osteogenic differentiation of BMSCs. Moreover, the CUR treatment upon BMSCs promoted the therapeutic effect of BMSC-derived exosomes.

Exosome derived from bone marrow mesenchymal stem cells pre-treated with curcumin alleviates osteoporosis by promoting osteogenic differentiation via regulating the METTL3/microRNA-320/RUNX2 signaling pathway

Yunhui Zhang [1+], Naiguo Wang [2+], Chenglin Zhang [3*]

1. Department of Orthopedics, Baoshan Hospital, Shuguang Hospital Affiliated to Shanghai University of Chinese Medicine, Shanghai 201999, China.
2. Department of Spinal surgery, Shandong Provincial Hospital Affiliated to Shandong University, Jinan 250021, Shandong, China.
3. Department of Orthopedics, Shanghai General Hospital, School of Medicine, Shanghai Jiaotong University, Shanghai 201620, China.

* Correspondence to: Chenglin Zhang,

Affiliation: Department of Orthopedics, Shanghai General Hospital, School of Medicine, Shanghai Jiaotong University, Shanghai 201620, China.

Address: 1878 N. Sichuan Rd, Shanghai, China, 200081

Email: boneresearch@126.com

+ Yunhui Zhang and Naiguo Wang contributed equally to this study.

Abstract

Background: Curcumin (CUR) was reported to stimulate the expression of methyltransferase - like 3 (METTL3), a potential new target for the replacement therapy of osteoporosis. Besides, marrow stem cells (MSC)-derived exosomes (EXO) were proven to improve osteoporosis by promoting the proliferation of osteoblasts. In this study, we aimed to study the effect of CUR and BMSC-derived exosomes in the treatment of osteoporosis. **Methods:** Microscopy was used to characterize exosomes derived from bone marrow stem cells (BMSCs). MicroCT was carried out to analyze the parameters of bone formation. Western blot was carried out to analyze the expression of surface markers on BMSC-derived exosomes and METTL3/Runt-related

transcription factor 2 (RUNX2) proteins under different conditions. Real-time PCR was used to assess the gene expression under different circumstances. **Results:** The exosomes derived from CUR-treated BMSCs showed an enhanced therapeutic effect on osteoporosis mice compared with exosomes derived from untreated BMSCs. Mechanistically, the effect of BMSC-derived exosomes on restoring the de-regulated expression of METTL3, miR-320 and RUNX2 was significantly enhanced by CUR treatment upon BMSCs. Besides, CUR treatment upon BMSCs showed an obvious effect on enhancing the stimulatory role of BMSC-derived exosomes in the expression of METTL3, miR-320, RUNX2, BGLAP and LAP in BMSCs. Furthermore, luciferase assay demonstrated that miR-320 was capable of suppressing the expression of RUNX2 through binding to the 3' UTR of RUNX2. **Conclusion:** Our study demonstrated that BMSC-derived exosomes could modulate the METTL3/miRNA-320/RUNX2 axis to attenuate osteoporosis by promoting osteogenic differentiation of BMSCs. Moreover, the CUR treatment upon BMSCs promoted the therapeutic effect of BMSC-derived exosomes.

Running title: CUR promoted the therapeutic effect of BMSC-derived exosomes

Key words: osteoporosis, curcumin, exosome, bone marrow stem cells, METTL3, miRNA-320, RUNX2

Introduction

As a bone condition featured by a weakening bone strength, lowered bone mass, damaged bone microstructures, as well as elevated brittleness of the bone, osteoporosis increases the danger of fracture. The risk of osteoporosis is increased over age [1, 2]. Along with the aging of the population worldwide, osteoporosis has turned into one of the most costly illness worldwide [3]. Osteoporosis can be classified into 2 groups, i.e., primary osteoporosis as well as secondary osteoporosis.

As a type of yellow polyphenolic substance originated from the extract of Curcuma longa, CUR was shown to possess anti-tumor, anti-inflammatory, anti-oxidant as well as anti-bacterial properties [4, 5]. Specifically, CUR was demonstrated to exhibit its anti-inflammatory effect via promoting the production of IL-10 and thus accordingly enhancing pathological interactions mediated by IL-10 [6]. Previous researches have presented that CUR may impair the function of

54 the tissue factors related to thrombotic diseases by inhibiting the aggregation of platelets or by
55 decreasing platelet activity [7]. In addition, many studies have found that CUR exerts a beneficial
56 effect in alleviating osteoporosis in both clinical as well as experimental models [8]. Previous
57 researches indicated that the combined administration of CUR and alendronate could enhance
58 bone mineral density (BMD) and modulate bone turnover markers in postmenopausal women
59 with osteoporosis [9]. And unlike all-trans retinoic acid (ATRA) which inhibited the mineralization
60 of differentiated cells during the later stages, CUR was proved to increase the osteogenic
61 differentiation capacity of BMSCs [10]. Moreover, the pre-administration of CUR into the BMSCs
62 could facilitate cell therapy in tissue repair treatment by improving mitochondrial function and
63 destabilizing HIF-1α, leading to the obstruction of potential hypoxia/reoxgenation injury [11, 12].
64 It was found that CUR prevented LPS-induced augmentation of SCD-1 and SREBP-1c mRNA
65 expression in the liver. Especially, CUR in the diet impacts the METTL14, METTL3, FTO, ALKBH5,
66 as well as YTHDF2 mRNA expression while increasing the content of m6A in piglet liver [13].

67 BMSC are recognized to release exosomes containing the molecules of over 150 types of different
68 miRNAs [14]. Numerous researches have revealed that exosomes play a primary role in the
69 therapeutic functions of BMSCs. In the cardiovascular system, the medium conditioned by BMSCs
70 improved heart functions [15]. Other studies illustrated that the mice treated with BMSC-derived
71 exosomes showed a reduced size of cardiac infarct ex vivo as well as in vivo [14, 16, 17]. The
72 BMSC exosomes derived from rat, human, as well as mouse have shown curative effects in a
73 range of various diseases [18]. It was also shown that hFOB 1.19 cell proliferation was enhanced
74 by Mesenchymal Stem Cells (MSC)-Exo, thus alleviating osteoporosis [19].

75 METTL3 was initially recognized as a primary methyltransferase in the process of methylation
76 and was later verified to exert an effect on the progression of certain cancers [20, 21]. It was
77 found that the METTL3 deletion in MSCs interrupts the normal cell cycle in mice to lead to
78 osteoporosis. In addition, the gain-of-function of METTL3 protects against postmenopausal
79 osteoporosis induced by estrogen deficiency [22]. Another study found that the methylation of
80 pre-miR-320 mediated by METTL3 promoted bone formation as well as the osteogenic
81 differentiation of BMSCs [23]. It was reported that by acting as a pro-osteogenic or an anti-
82 osteoporotic factor, METTL3 could maintain a high level of RUNX2 expression via direct

methylation of RUNX2 as well as indirect up-regulation of RUNX2 expression through pre-miR-320 methylation [23]. And RUNX2, as previously reported, acts as a transcript factor specific to osteoblast which plays a critical role in the differentiation of MSCs into osteoblasts [24, 25]. RUNX2 could regulate osteoblast differentiation by triggering the expression of several major bone matrix genes during the early stages of osteoblast differentiation [24].

The over-expression of METTL3 has been reported as a potential approach of replacement therapy for the treatment of osteoporosis [23]. Moreover, it was also demonstrated that CUR affected the expression of METTL3 in the pathogenesis of LPS-induced liver injury [13]. Moreover, MSC-derived exosomes were proven to improve osteoporosis by promoting the proliferation of osteoblasts [19]. It has been shown that encapsulated with exosome will improve the delivery of curcumin [26]. On the other hand, combination with curcumin will enhance the therapeutic effect of exosomes [27]. Based on the above-mentioned evidences, we hypothesized that curcumin may promoted expression of METTL3 which subsequently downregulated expression of miR-320 by hypermethylation the promoter region and as a result, the expression of RUNX3, a direct target gene of miR-320, could be upregulated. Furthermore, pretreatment with curcumin will enhance the therapeutic effect of BMMSCs-derived exosomes in the treatment of osteoporosis. To test the hypothesis, we studied the effect of CUR and BMSC-derived exosomes in rat and cellular models of osteoporosis. Expression of METTL3, miR-320 and RUNX2 was investigated in vivo and in vitro to unveil the signaling pathway underlying the therapeutic effect of CUR on osteoporosis.

Materials and Methods

Animal and treatment

C57BL/6 mice with an average age of 8 weeks old were acquired from our animal center. All mice were kept in a specific pathogen-free (SPF) environment in the animal facility of our institution. All animal experiments in this study were approved by the Institutional Animal Care and Use Committee and were conducted in strict compliance with the “Guide for the Care and Use of Laboratory Animals” published by the US National Institutes of Health (NIH).. After 7 days of adaptation, the mice were divided into 4 groups, i.e., 1. Sham group (mice undergoing sham

111 operation); 2. Osteoporosis group (mice induce of osteoporosis); 3. Osteoporosis + EXO group
112 (mice induced of osteoporosis and then treated with EXO extracted from untreated BMSCs); and
113 4. Osteoporosis + EXO-CUR group (mice induced of osteoporosis and then treated with EXO
114 extracted from BMSCs treated with CUR).

115 **Mouse Model of Osteoporosis**

116 The C57BL/6 mice with an average age of 8 weeks old were used to create the osteoporosis model.
117 In brief, the model mice were subject to bilateral ovariectomy by exposing the bilateral ovaries
118 and removing nearby adipose tissues. The mice in the sham group also underwent the
119 ovariectomy operation without removing tissues. After the operation, all mice in the groups were
120 kept alive for 8 weeks before they were killed to harvest tissue samples for subsequent analyses.
121 The animal in each group were evaluated by microCT.

122 **Primary Cell Extraction and Culture**

123 In this study, BMSCs were isolated from femur and tibia bones collected from Sprague Dawley
124 (SD) rats under aseptic conditions. In brief, before the collection of tibia and femur bones, the
125 rats were killed via cervical vertebra dislocation. Then, BMSCs were isolated via rinsing the cavity
126 of bone marrow with a Modified Eagle Medium (MEM, Gibco, Rockville, MD) containing a higher
127 glucose content. Subsequently, the collected BMSCs which cultured in a Dulbecco's Modified
128 Eagle Medium (DMEM, Gibco, Rockville, MD) added with 10% of fetal bovine serum, 1% penstrep
129 as well as 1% L-glutamine (HyClone, South Logan, UT). The culture conditions were 37 °C, 5% CO_2
130 and saturated humidity. After the confluence of BMSCs reached 80%, they were trypsinized
131 (Beyotime, Shanghai, China) for sub-culture. BMSCs between 2-5 passages were used for further
132 analyses. In the EXO-CUR group, the BMSCs were incubated with CUR (1 μM) for 24 hours before
133 the isolation of EXO.

134 **Exosome Extraction**

135 To remove the residual cells, the cell supernatants of BMSCs were collected and centrifuged at
136 300 g for 10 min and 2000 g for 15 min at 4°C. To remove the cell debris, a subsequent
137 centrifugation at 12000 g for 30 min at 4°C was conducted. Particles larger than 200 nm was

138 removed by 0.22 μm filtration. And the cell suspensions were centrifuged at 100000 g for 2 h at
139 4°C again before the cell supernatants were discarded. For the final re-suspension step, PBS
140 buffer were applied before a preservation at -80°C.

141 **RNA isolation and real-time PCR**

142 In this study, real-time PCR was utilized to assay the relative expression of METTL3, miR-320,
143 RUNX2 mRNA, BGLAP mRNA, and TOUR mRNA in each sample. In brief, the collected tissue and
144 cell samples were lysed using a Trizol reagent (Invitrogen, Carlsbad, CA) in accordance with the
145 standard protocols provided in the manufacturer's instruction manual to isolate total RNA, which
146 was then converted to cDNA by using a cDNA RT assay kit (TAKARA, Tokyo, Japan) in accordance
147 with the standard protocols provided in the manufacturer's instruction manual. In the next step,
148 the cDNA was used as the template for real time PCR reactions, where were done by utilizing a
149 SYBR Premix EX Taq assay kit (TARKARA, Tokyo, Japan) on a PRISM 7900HT real time PCR
150 instrument (ABI, Foster City, CA) in accordance with the standard protocols provided in the
151 manufacturer's instruction manual. Finally, the relative expression of METTL3, miR-320, RUNX2
152 mRNA, BGLAP mRNA, and TOUR mRNA in each sample was calculated by utilizing the $2^{-\Delta\Delta Ct}$
153 method.

154 **Cell culture and transfection**

155 BMSCs and MG63 cells were bought from ATCC and cultured in DMEM under conditions
156 suggested by the manufacturer. Then, after the cell confluence reached 80%, the cells were
157 divided into 3 groups, i.e., 1. NC group (cells treated with PBS only); 2. CUR group (cells treated
158 with CUR); and 3. EXO-CUR group (cells treated with CUR-carrying EXO). Then, the cells were
159 treated under corresponding conditions for 48 h before the cells were harvested for target gene
160 analysis. Similarly, BMSCs and MG63 cells were divided into 2 groups, i.e., 1. NC siRNA group
161 (cells treated with a scramble control siRNA); 2. METTL3 siRNA group (cells treated with METTL3
162 siRNA), and the target gene analysis was done after the cells were transfected with corresponding
163 siRNAs for 48 h using Lipofectamine 2000 (Invitrogen, Carlsbad, CA) in accordance with the
164 standard protocols provided in the manufacturer's instruction manual.

165 **Vector construction, mutagenesis, and luciferase assay**

166 Our binding site screening found that miR-320 could potentially bind to the 3' UTR of RUNX2.
167 Therefore, to clarify the regulatory relationship between the expression of miR-320 and RUNX2,
168 luciferase vectors containing wild type and mutant RUNX2 were established: First, the wild type
169 3' UTR of RUNX2 containing the miR-320 binding site was amplified and cloned into a pcDNA3.1
170 vector (Promega, Madison, WI) downstream of the luciferase gene to create the wild type vector
171 for the 3' UTR of RUNX2. At the same time, mutagenesis was carried out to generate one site-
172 directed mutation in the miR-320 binding site located in the 3' UTR of RUNX2, and the mutant
173 fragment of 3' UTR of RUNX2 was also amplified and cloned into another pcDNA3.1 vector to
174 generate the mutant type vector for the 3' UTR of RUNX2. In the next step, BMSCs and MG63
175 were co-transfected with mutant type/wild type vectors for the 3' UTR of RUNX2 together with
176 miR-320 mimics or a control using Lipofectamine 2000, and the luciferase activity of transfected
177 cells was measured at 48 h after the start of co-transfection with a Dual-luciferase assay kit
178 (Promega, Madison, WI) on a luminometer in accordance with the standard protocols provided
179 in the manufacturer's instruction manual.

180 **Western blot analysis**

181 Cell and tissue samples were first lysed using a RIPA lysis system (Beyotime, Shanghai, China) in
182 accordance with the standard protocols provided in the manufacturer's instruction manual. Then,
183 20 μg of proteins from each sample were fractionated by using a 10% SDS-PAGE gel, and the
184 fractionated proteins were electro-transferred onto a polyvinylidene fluoride membrane
185 (Millipore, Burlington, MA), which was blocked by using 5% non-fat, washed with TBST, and
186 treated overnight (4°C) with anti-METTL3 and anti-RUNX2 primary antibodies (Abcam,
187 Cambridge, MA) in accordance with the standard conditions provided in the manufacturer's
188 instruction manual, followed by further incubation against HRP-conjugated secondary antibodies
189 (Santa Cruz Biotechnology, Santa Cruz, CA) at ambient temperature for 2 h. Finally, the protein
190 bands were developed by making use of an enhanced chemiluminescence reagent (Thermo
191 Scientific, Waltham, MA) in accordance with the standard protocols provided in the
192 manufacturer's instruction manual, and the relative expression of METTL3 and RUNX2 proteins
193 in each sample was semi-quantified by utilizing a ChemiDoc XRS+ machine (Bio-Rad laboratories,
194 Hercules, CA) and the ImageJ 1.40 software.

195 **Immunohistochemistry**

196 For immunofluorescence assays, the samples were made into 4 μm thick slides and blocked with
197 5% BSA for 1 h before they were incubated successively with anti-METTL3 primary antibodies,
198 and suitable AlexaFluor 568-conjugated secondary antibodies (all antibodies were obtained from
199 Abcam, Cambridge, MA and used in accordance with the standard conditions shown in the
200 manufacturer's instruction manual). After counterstaining with DAPI, the positive expression of
201 METTL3 protein in each sample was evaluated under an Axio Observer Z1 microscope coupled
202 with a Zeiss LSM 5 imaging system (Carl Zeiss, Oberkochen, Germany).

203 **Statistical analysis**

204 All data analyses were done by making use of GraphPad Prism 6.0 software (GraphPad, San Diego,
205 CA). Two-tailed Student's t-tests were used for the comparison between two groups. All data
206 were presented as mean ± standard deviation (SD) and each observation was repeated in
207 triplicate. P-value < 0.05 was taken into consideration as statistically significant.

208 **Results**

209 **Isolation and characterization of BMSC-derived exosomes.**

210 BMSCs were cultured for three days and their morphology exhibited a vortex distribution and a
211 spindle like shape under a microscope (Fig.1A). Exosomes were isolated from BMSCs and the
212 shape of exosomes was evaluated using electron microscopy, and the results showed exosomes
213 as round bubbles with a 40 nm diameter (Fig.1B). Furthermore, Western blot was carried out to
214 analyze the expression of CD9, CD63 and CD81 in the supernatant of BMSCs as well as in BMSC-
215 derived exosomes. The expression of CD9, CD63 and CD81 was significantly elevated in BMSC-
216 derived exosomes when compared with that in the supernatant of BMSCs (data not shown).

217 **CUR treatment remarkably enhanced the therapeutic effect of BMSC-derived exosomes in mice**
218 **with osteoporosis .**

219 In order to evaluate the therapeutic effect of CUR upon BMSC-derived exosomes, mice models
220 of osteoporosis was established. MicroCT was used to measure the Bone volume/Tissue volume

221 ratio (BV/TV), BMD, Trabecular number (Tb.N), Trabecular thickness (Tb.Th) and Trabecular
222 separation (Tb.Sp) of the osteoporosis mice treated with different therapeutic strategies.
223 Accordingly, the BV/TV, BMD, Tb.N and Tb.Th were remarkably decreased in osteoporosis mice,
224 while BMSC-derived exosomes exerted a notable effect on restoring the values of BV/TV, BMD,
225 Tb.N and Tb.Th in osteoporosis mice. Moreover, the exosomes derived from CUR-treated BMSCs
226 more significantly exerted an promoting effect on BV/TV (Fig.2A, Fig.2F), BMD (Fig.2B, Fig.2F),
227 Tb.N (Fig.2C, Fig.2F), and Tb.Th (Fig.2D, Fig.2F) in osteoporosis mice. On the contrary, CUR
228 treatment obviously enhanced the effect of BMSC-derived exosomes on suppressing the
229 abnormally increased Tb.Sp value in osteoporosis mice (Fig.2E, Fig.2F).

230 **CUR treatment effectively strengthened the capability of BMSC-derived exosomes in**
231 **maintaining the expression of METTL3, miR-320 and RUNX2 in osteoporosis mice.**

232 To gain a deep insight into the molecular mechanism underlying the therapeutic effect of CUR
233 and BMSC-derived exosomes, we performed PCR, Western blot and immunohistochemistry to
234 analyze the expression of METTL3, RUNX2 and miR-320 in osteoporosis mice treated under
235 different conditions. Accordingly, the expression of METTL3 mRNA and protein was apparently
236 suppressed in osteoporosis mice. And CUR treatment upon BMSCs obviously promoted the
237 capability of BMSC-derived exosomes in maintaining the suppressed expression of METTL3
238 mRNA (Fig.3A) and protein (Fig.3B, Fig.4) in osteoporosis mice. On the contrary, the activated
239 expression of miR-320 in osteoporosis mice was effectively repressed by the exosomes derived
240 from CUR-treated BMSCs (Fig.3C). Besides, the repressed expression of RUNX2 mRNA (Fig.3D)
241 and protein (Fig.3E) in osteoporosis mice was effectively maintained by the exosomes derived
242 from CUR-treated BMSCs.

243 **BMSC-derived exosomes remarkably enhanced the effect of CUR on regulating the expression**
244 **of METTL3, miR-320, RUNX2, BGLAP and LAP in BMSCs cells.**

245 Furthermore, we treated BMSCs cells with CUR alone or in combination with BMSC-derived
246 exosomes to evaluate their effect on the expression of METTL3, miR-320, RUNX2, BGLAP and LAP.
247 As shown in Fig.5, BMSC-derived exosomes showed a remarkable potential in enhancing the
248 effect of CUR on increasing the expression of METTL3 mRNA (Fig.5A), METTL3 protein (Fig.5B),

249 RUNX2 mRNA (Fig.5D), RUNX2 protein (Fig.5E), BGLAP mRNA (Fig.5F) and LAP mRNA (Fig.5G) as
250 well as on decreasing the expression of miR-320 in BMSCs cells (Fig.5C).

251 **METTL3 siRNA notably repressed the expression of METTL3, RUNX2, BGLAP, and LAP, and**
252 **activated the expression of miR-320 in BMSCs cells.**

253 BMSCs cells were treated with METTL3 siRNA and the expression of METTL3, miR-320, RUNX2,
254 BGLAP and LAP was analyzed using real-time PCR and Western blot. The expression of METTL3
255 mRNA (Fig.6A), METTL3 protein (Fig.6B), RUNX2 mRNA (Fig.6D), RUNX2 protein (Fig.6E), BGLAP
256 mRNA (Fig.6F) and LAP mRNA (Fig.6G) was evidently suppressed by METTL3 siRNA in BMSCs cells.
257 The expression of miR-320 was increased in BMSCs cells treated with METTL3 siRNA (Fig.6C).

258 **MiR-320 inhibited the expression of RUNX2 through binding to the 3' UTR of RUNX2.**

259 Binding site screening found that miR-320 could potentially bind to the 3' UTR of RUNX2 (Fig.7A).
260 Luciferase vectors containing wild type and mutant RUNX2 were established and transfected into
261 BMSCs and MG63 cells along with miR-320. The luciferase activity of wild type RUNX2 vector was
262 significantly inhibited in BMSCs (Fig.7B) and MG63 (Fig.7C) cells, indicating that miR-320
263 suppressed the expression of RUNX2. Moreover, we examined the expression of RUNX2 in BMSCs
264 and MG63 cells treated with different concentrations of a miR-320 precursor. The expression of
265 RUNX2 mRNA was apparently suppressed in miR-320-treated BMSCs (Fig.7D) and MG63 (Fig.7E)
266 cells.

267 In summary, our study demonstrated that BMSC-derived exosomes and CUR jointly enhanced
268 the expression of METTL3, which down-regulated the expression of miR-320, resulting in the up-
269 regulation of RUNX2. As a result, osteogenic differentiation was enhanced to alleviate
270 osteoporosis (Fig.8).

271 **Discussion**

272 In this study, we harvested exosomes from bone marrow stem cells and treated osteoporosis
273 mice with the combination of CUR and BMSC-derived exosomes. The therapeutic effect of CUR
274 on osteoporosis was remarkably elevated by BMSC-derived exosomes. In addition, we performed
275 real-time PCR, Western blot and IHC to examine the expression of METTL3, miR-320 and RUNX2

276 at both the mRNA and protein levels in osteoporosis mice treated under different conditions.
277 BMSC-derived exosomes strengthened with CUR significantly restored the expression of METTL3,
278 miR-320 and RUNX2 in osteoporosis mice. As a type of phenolic substance separated from
279 Curcuma longa, CUR exhibits certain anti-inflammatory, anti-tumor and anti-mutagenic effects
280 [28, 29]. Studies have suggested that CUR affects both fat accumulation as well as bone health in
281 the body. In addition, CUR may cause the apoptosis of osteoclasts while preventing the growth
282 of osteoclasts by decreasing RANKL expression in BMSCs [29, 30]. It was also found that CUR
283 reduced in vivo osteoporosis induced by DXM [31].

284 It was revealed that BMSC proliferation on modified surfaces of LC was significantly increased by
285 0.05 mg/ml of BMP2. Similarly, osteonectin expression was increased by BMP2 on LC as well as
286 UDMA surfaces [32]. Surprisingly, a recent research suggested that the accumulation of m6A in
287 both mouse and human was regulated by mRNAs through their selective binding to METTL3 [13,
288 33]. Consistently, Vashisht et al. recently suggested that CUR loaded in exosomes is not only
289 resistant to enzymatic digestion, but also shows elevated permeability in the digestive tract [26,
290 34, 35]. Certain evidence suggested that MSC-derived exosomes as well as exosome-like
291 nanoparticles derived from edible plants can also resist enzymatic digestion [26, 36].

292 A previous research presented that exosomal MALAT1 in BMSCs might contribute to increased
293 osteogenic activity as well as relieved osteoporosis symptoms through functioning as a sponge
294 of miR-34c to upregulate the expression of SATB2 [37]. Hence, it was found that nearly 75% of
295 super-enhancer RNAs (seRNAs) show the peaks of m6A. In addition, the level of m6A methylation
296 in seRNAs was decreased in Mettl3 KO models [38]. Furthermore, pre-miR-320 methylation in
297 the nucleus results in the down-regulation of miR-320 expression in the cytoplasm, contributing
298 to the osteogenic potential of METTL3 [19]. Additionally, the down-regulation of miR-320 rescued
299 the bone mass loss shown in METTL3 +/- knockout [23]. In this study, we treated BMSCs cells
300 with CUR alone or in the combination with BMSC-derived exosomes. BMSC-derived exosomes
301 significantly enhanced the role of CUR in promoting the expression of METTL3 and RUNX2 mRNA
302 and in suppressing the expression of miR-320 in BMSCs cells.

303 The bioinformatics studies showed that the 3'-UTR of RUNX2 contains four miR-320 binding sites.
304 The interaction of RUNX2 3'-UTR and miR-320 is also specific, as mutations in the 3'-UTR of
305 RUNX2 blocked the binding between miR-320 and RUNX2 3'-UTR [39]. In this study, we
306 performed luciferase assay to explore the inhibitory role of miR-320 in the expression of RUNX2.
307 The luciferase activity of wild type RUNX2 was significantly repressed by miR-320 in BMSCs and
308 MG63 cells.

309 RUNX2 belongs to the family of RUNT related transcription factors that are essential in the course
310 of skeletal development during embryogenesis. RUNX2 is also recognized for its oncogenic
311 functions. In fact, numerous studies revealed that the dysregulation of RUNX2 leads to tumor
312 progression as well as tumor invasion [40]. Additionally, RUNX2 was found to be involved in bone
313 development as well as hypertrophic differentiation of chondrocytes [41, 42]. Past studies
314 showed that the adipocytic differentiation of MSCs was inhibited by RUNX2 [43]. It was also
315 shown that the differentiation of MSCs into osteoblasts is the main pathway for bone formation
316 [39]. Runx2 can activate and regulate osteogenesis via many different signaling pathways, such
317 as the TGF-β1, BMP, Wnt, Hedgehog, as well as NELL-1 signaling pathways [26, 27]. The mice
318 carrying the homozygous Runx2 −/− mutations lack differentiated osteoblasts upon birth [44, 45].
319 While Runx2 does not act as a crucial regulator in the differentiation of adipocytes, its role in
320 enhancing osteogenesis might affect the differentiation of adipocyte lineages [46]. In addition,
321 we treated BMSCs cells with METTL3 siRNA and checked the expression of METTL3, miR-320,
322 RUNX2, BGLAP and LAP in BMSCs cells. The expression of METTL3, RUNX2, BGLAP and LAP was
323 notably suppressed by METTL3 siRNA, while the expression of miR-320 was apparently enhanced
324 by METTL3 siRNA in BMSCs cells.

325 However, our study is limited by the lack of clinical validation. Although a conclusion that
326 exosomes derived from CUR-treated BMSCs could promote the therapeutic effect of CUR, future
327 clinical validation should be conducted.

328 **Conclusion**

329 In conclusion, our study demonstrated that BMSC-derived exosomes could modulate the
330 signaling pathway of METTL3/miRNA-320/RUNX2 to attenuate osteoporosis by promoting

331 osteogenic differentiation of BMSCs. Moreover, exosomes derived from CUR-treated BMSCs
332 promoted the therapeutic effect of CUR.

333 **Conflict of interest**

334 None

335 **Author Contributions Statement**

336 Y.H.Z and C.L.Z wrote the main manuscript text and N.G.W and C.L.Z prepared figures 1-7. All
337 authors reviewed the manuscript

338 **Statement**

339 The data that support the findings of this study are available from the corresponding author up
340 on reasonable request.

341 **Figure legends**

342 **Fig.1**

343 Characterization of exosomes isolated from bone marrow stem cells.

344 A: The primary bone marrow stem cells showed a long spindle shape.

345 B: Representative images of BMSC-derived exosomes observed under an electron microscope.

346 **Fig.2**

347 CUR treatment strengthened the therapeutic effect of BMSC-derived exosomes on osteoporosis
348 mice (* P-value < 0.05 vs. SHAM group; ** P-value < 0.05 vs. OSTEOPOROSIS group; # P-value <
349 0.05 vs. OSTEOPOROSIS + CUR group).

350 A: CUR treatment enhanced the capability of BMSC-derived exosomes in restoring the Bone
351 volume/Tissue volume ratio in osteoporosis mice.

352 B: CUR treatment enhanced the capability of BMSC-derived exosomes in restoring the Bone
353 mineral density in osteoporosis mice.

354 C: CUR treatment enhanced the capability of BMSC-derived exosomes in restoring the Trabecular
355 number in osteoporosis mice.

356 D: CUR treatment enhanced the capability of BMSC-derived exosomes in restoring the Trabecular
357 thickness in osteoporosis mice.

358 E: CUR treatment enhanced the capability of BMSC-derived exosomes in restoring the Trabecular
359 separation in osteoporosis mice.

360 F: Representative micro-CT images of mice groups.

361 **Fig.3**

362 CUR treatment enhanced the capability of BMSC-derived exosomes in maintaining the expression
363 of METTL3, miR-320 and RUNX2 in osteoporosis mice (* P-value < 0.05 vs. Sham group; ** P-
364 value < 0.05 vs. Osteoporosis group; # P-value < 0.05 vs. Osteoporosis + EXO group).

365 A: CUR treatment enhanced the capability of BMSC-derived exosomes in maintaining the
366 expression of METTL3 mRNA in osteoporosis mice.

367 B: CUR treatment enhanced the capability of BMSC-derived exosomes in maintaining the
368 expression of METTL3 protein in osteoporosis mice.

369 C: CUR treatment enhanced the capability of BMSC-derived exosomes in maintaining the
370 expression of miR-320 in osteoporosis mice.

371 D: CUR treatment enhanced the capability of BMSC-derived exosomes in maintaining the
372 expression of RUNX2 mRNA in osteoporosis mice.

373 E: CUR treatment enhanced the capability of BMSC-derived exosomes in maintaining the
374 expression of RUNX2 protein in osteoporosis mice.

375 **Fig.4**

376 Immunohistochemistry analysis showed that CUR treatment enhanced the capability of BMSC-
377 derived exosomes in maintaining the expression of METTL3 protein in osteoporosis mice.

378 **Fig.5**

379 Exosomes derived from CUR-treated BMSCs strengthened the ability of CUR in altering the
380 expression of METTL3, miR-320, RUNX2, BGLAP and LAP in BMSCs cells (* P-value < 0.05 vs. NC
381 group; ** P-value < 0.05 vs. CUR group).

382 A: Exosomes derived from CUR-treated BMSCs strengthened the effect of CUR in promoting the
383 expression of METTL3 mRNA in BMSCs cells.

384 B: Exosomes derived from CUR-treated BMSCs strengthened the effect of CUR in promoting the
385 expression of METTL3 protein in BMSCs cells.

386 C: Exosomes derived from CUR-treated BMSCs strengthened the effect of CUR in suppressing the
387 expression of miR-320 in BMSCs cells.

388 D: Exosomes derived from CUR-treated BMSCs strengthened the effect of CUR in promoting the
389 expression of RUNX2 mRNA in BMSCs cells.

390 E: Exosomes derived from CUR-treated BMSCs strengthened the effect of CUR in promoting the
391 expression of RUNX2 protein in BMSCs cells.

392 F: Exosomes derived from CUR-treated BMSCs strengthened the effect of CUR in promoting the
393 expression of BGLAP mRNA in BMSCs cells.

394 G: Exosomes derived from CUR-treated BMSCs strengthened the effect of CUR in promoting the
395 expression of LAP mRNA in BMSCs cells.

396 **Fig.6**

397 METTL3 siRNA transfection altered the expression of METTL3, miR-320, RUNX2, BGLAP and LAP
398 in BMSCs cells (* P-value < 0.05 vs. NC siRNA group).

399 A: The expression of METTL3 mRNA was suppressed by METTL3 siRNA in BMSCs cells.

400 B: The expression of METTL3 protein was suppressed by METTL3 siRNA in BMSCs cells.

401 C: The expression of miR-320 was increased by METTL3 siRNA in BMSCs cells.

402 D: The expression of RUNX2 mRNA was suppressed by METTL3 siRNA in BMSCs cells.

403 E: The expression of RUNX2 protein was suppressed by METTL3 siRNA in BMSCs cells.

404 F: The expression of BGLAP mRNA was suppressed by METTL3 siRNA in BMSCs cells.

405 G: The expression of LAP mRNA was suppressed by METTL3 siRNA in BMSCs cells.

406 **Fig.7**

407 MiR-320 suppressed the expression of RUNX2 through binding to its 3' UTR.

408 A: Sequence analysis indicated that miR-320 could potentially bind to the 3' UTR of RUNX2.

409 B: The luciferase activity of wild type RUNX2 was remarkably suppressed by miR-320 in BMSCs
410 cells (* P-value < 0.05 vs. control group).

411 C: The luciferase activity of wild type RUNX2 was remarkably suppressed by miR-320 in MG63
412 cells (* P-value < 0.05 vs. control group).

413 D: The expression of RUNX2 mRNA was repressed by miR-320 precursors in a dose dependent
414 manner in BMSCs cells (* P-value < 0.05 vs. scramble group).

415 E: The expression of RUNX2 mRNA was repressed by miR-320 precursors in a dose dependent
416 manner in MG63 cells (* P-value < 0.05 vs. scramble group).

417 **Fig.8**

418 Schematic illustration of the study.

419 **References**

420 1. Pietschmann, P., et al., *Osteoporosis: an age-related and gender-specific disease--a mini-*
421 *review.* Gerontology, 2009. **55**(1): p. 3-12.
422 2. Mulder, J.E., N.S. Kolatkar, and M.S. LeBoff, *Drug insight: Existing and emerging therapies*
423 *for osteoporosis.* Nat Clin Pract Endocrinol Metab, 2006. **2**(12): p. 670-80.
424 3. Burge, R., et al., *Incidence and economic burden of osteoporosis-related fractures in the*
425 *United States, 2005-2025.* J Bone Miner Res, 2007. **22**(3): p. 465-75.
426 4. Toden, S., et al., *Essential turmeric oils enhance anti-inflammatory efficacy of curcumin in*
427 *dextran sulfate sodium-induced colitis.* Sci Rep, 2017. **7**(1): p. 814.

428 5. Shlar, I., S. Droby, and V. Rodov, *Modes of antibacterial action of curcumin under dark and*
429 *light conditions: A toxicoproteomics approach.* J Proteomics, 2017. **160**: p. 8-20.
430 6. Mollazadeh, H., et al., *Immune modulation by curcumin: The role of interleukin-10.* Crit
431 Rev Food Sci Nutr, 2019. 59(1): p. 89-101. Mollazadeh, H., et al., *Immune modulation by*
432 *curcumin: The role of interleukin-10.* Crit Rev Food Sci Nutr, 2019. **59**(1): p. 89-101.

433 7. Pan, C.J., et al., *Improved blood compatibility of rapamycin-eluting stent by incorporating*
434 *curcumin.* Colloids Surf B Biointerfaces, 2007. **59**(1): p. 105-11.
435 8. Mawani, Y. and C. Orvig, *Improved separation of the curcuminoids, syntheses of their rare*
436 *earth complexes, and studies of potential antiosteoporotic activity.* J Inorg Biochem, 2014.
437 **132**: p. 52-8.
438 9. Khanizadeh, F., et al., *Combination therapy of curcumin and alendronate modulates bone*
439 *turnover markers and enhances bone mineral density in postmenopausal women with*
440 *osteoporosis*. Arch Endocrinol Metab, 2018. **62**(4): p. 438-45.
441 10. Ahmed, M. F., et al., *Comparison between curcumin and all-trans retinoic acid in the*
442 *osteogenic differentiation of mouse bone marrow mesenchymal stem cells*. Exp Ther Med,
443 2019. **17**(5): p. 4154–66.
444 11. Wang, H., et al., *Curcumin pretreatment protects against hypoxia/reoxgenation injury via*
445 *improvement of mitochondrial function, destabilization of HIF-1α and activation of Epac1-*
446 *Akt pathway in rat bone marrow mesenchymal stem cells*. Biomed Pharmacother, 2019.
447 **109**: p. 1268-75.

448 12. Sahebkar , A., et al., *Curcumin downregulates human tumor necrosis factor-α levels: A*
449 *systematic review and meta-analysis of randomized controlled trials*. Pharmacol Res, 2016.
450 **107**: p. 234-42.

451 13. Lu, N., et al., *Curcumin Attenuates Lipopolysaccharide-Induced Hepatic Lipid Metabolism*
452 *Disorder by Modification of m(6) A RNA Methylation in Piglets.* Lipids, 2018. **53**(1): p. 53-
453 63.
454 14. Xie, Y., et al., *Derivation and characterization of goat fetal fibroblast cells induced with*
455 *human telomerase reverse transcriptase.* In Vitro Cell Dev Biol Anim, 2013. **49**(1): p. 8-14.

456 15. Timmers, L., et al., *Reduction of myocardial infarct size by human mesenchymal stem cell*
457 *conditioned medium.* Stem Cell Res, 2007. **1**(2): p. 129-37.
458 16. Ebrahim, N., et al., *Mesenchymal Stem Cell-Derived Exosomes Ameliorated Diabetic*
459 *Nephropathy by Autophagy Induction through the mTOR Signaling Pathway.* Cells, 2018.
460 **7**(12).
461 17. Furuta, T., et al., *Mesenchymal Stem Cell-Derived Exosomes Promote Fracture Healing in*
462 *a Mouse Model.* Stem Cells Transl Med, 2016. **5**(12): p. 1620-1630.
463 18. Katsuda, T. and T. Ochiya, *Molecular signatures of mesenchymal stem cell-derived*
464 *extracellular vesicle-mediated tissue repair.* Stem Cell Res Ther, 2015. **6**: p. 212.
465 19. Zhao, P., et al., *Exosomes derived from bone marrow mesenchymal stem cells improve*
466 *osteoporosis through promoting osteoblast proliferation via MAPK pathway.* Eur Rev Med
467 Pharmacol Sci, 2018. **22**(12): p. 3962-3970.
468 20. Visvanathan, A., et al., *Essential role of METTL3-mediated m(6)A modification in glioma*
469 *stem-like cells maintenance and radioresistance.* Oncogene, 2018. **37**(4): p. 522-533.
470 21. Wen, J., et al., *Zc3h13 Regulates Nuclear RNA m(6)A Methylation and Mouse Embryonic*
471 *Stem Cell Self-Renewal.* Mol Cell, 2018. **69**(6): p. 1028-1038 e6.
472 22. Wu, Y., et al., *Mettl3-mediated m(6)A RNA methylation regulates the fate of bone marrow*
473 *mesenchymal stem cells and osteoporosis.* Nat Commun, 2018. **9**(1): p. 4772.
474 23. Yan, G., et al., *m(6)A Methylation of Precursor-miR-320/RUNX2 Controls Osteogenic*
475 *Potential of Bone Marrow-Derived Mesenchymal Stem Cells.* Mol Ther Nucleic Acids, 2020.
476 **19**: p. 421-436.
477 24. Komori, T., *Regulation of osteoblast differentiation by Runx2.* Adv Exp Med Biol, 2010. **658**:
478 p. 43-9.
479 25. Pratap, J., et al., *Runx2 transcriptional activation of Indian Hedgehog and a downstream*
480 *bone metastatic pathway in breast cancer cells.* Cancer Res, 2008. **68**(19): p. 7795-802.
481 26. Vashisht, M., et al., *Curcumin Encapsulated in Milk Exosomes Resists Human Digestion*
482 *and Possesses Enhanced Intestinal Permeability in Vitro.* Appl Biochem Biotechnol, 2017.
483 **183**(3): p. 993-1007.

484 27. Oskouie, M.N., et al., *Therapeutic use of curcumin-encapsulated and curcumin-primed*
485 *exosomes.* J Cell Physiol, 2019. **234**(6): p. 8182-91.
486 28. Aggarwal, B.B., et al., *Curcumin: the Indian solid gold.* Adv Exp Med Biol, 2007. **595**: p. 1-
487 75.
488 29. Bharti, A.C., Y. Takada, and B.B. Aggarwal, *Curcumin (diferuloylmethane) inhibits receptor*
489 *activator of NF-kappa B ligand-induced NF-kappa B activation in osteoclast precursors and*
490 *suppresses osteoclastogenesis.* J Immunol, 2004. **172**(10): p. 5940-7.
491 30. Ozaki, K., et al., *Stimulatory effect of curcumin on osteoclast apoptosis.* Biochem
492 Pharmacol, 2000. **59**(12): p. 1577-81.
493 31. Chen, Z., et al., *Curcumin alleviates glucocorticoid-induced osteoporosis through the*
494 *regulation of the Wnt signaling pathway.* Int J Mol Med, 2016. **37**(2): p. 329-38.
495 32. Florian, B., et al., *MSC differentiation on two-photon polymerized, stiffness and BMP2*
496 *modified biological copolymers.* Biomed Mater, 2019. **14**(3): p. 035001.
497 33. Chen, T., et al., *m(6)A RNA methylation is regulated by microRNAs and promotes*
498 *reprogramming to pluripotency.* Cell Stem Cell, 2015. **16**(3): p. 289-301.
499 34. Liao, Y., et al., *Human milk exosomes and their microRNAs survive digestion in vitro and*
500 *are taken up by human intestinal cells.* Mol Nutr Food Res, 2017. **61**(11).
501 35. Ma, H., et al., *Differential expression study of circular RNAs in exosomes from serum and*
502 *urine in patients with idiopathic membranous nephropathy.* Arch Med Sci, 2019. **15**(3): p.
503 738–53.
504 36. Agrawal, A.K., et al., *Milk-derived exosomes for oral delivery of paclitaxel.* Nanomedicine,
505 2017. **13**(5): p. 1627-1636.
506 37. Yang, X., et al., *LncRNA MALAT1 shuttled by bone marrow-derived mesenchymal stem*
507 *cells-secreted exosomes alleviates osteoporosis through mediating microRNA-34c/SATB2*
508 *axis.* Aging (Albany NY), 2019. **11**(20): p. 8777-8791.
509 38. Liu, J., et al., *N (6)-methyladenosine of chromosome-associated regulatory RNA regulates*
510 *chromatin state and transcription.* Science, 2020. **367**(6477): p. 580-586.
511 39. Hamam, D., et al., *microRNA-320/RUNX2 axis regulates adipocytic differentiation of*
512 *human mesenchymal (skeletal) stem cells.* Cell Death Dis, 2014. **5**: p. e1499.

513 40. Sancisi, V., et al., *RUNX2 expression in thyroid and breast cancer requires the cooperation*
514 *of three non-redundant enhancers under the control of BRD4 and c-JUN.* Nucleic Acids Res,
515 2017. **45**(19): p. 11249-11267.
516 41. Yu, S., et al., *Osteogenic differentiation of C2C12 myogenic progenitor cells requires the*
517 *Fos-related antigen Fra-1 - a novel target of Runx2.* Biochem Biophys Res Commun, 2013.
518 **430**(1): p. 173-8.
519 42. Li, H., et al., *A novel microRNA targeting HDAC5 regulates osteoblast differentiation in*
520 *mice and contributes to primary osteoporosis in humans.* J Clin Invest, 2009. **119**(12): p.
521 3666-77.
522 43. Kobayashi, H., et al., *Multilineage differentiation of Cbfa1-deficient calvarial cells in vitro.*
523 Biochem Biophys Res Commun, 2000. **273**(2): p. 630-6.
524 44. Otto, F., et al., *Cbfa1, a candidate gene for cleidocranial dysplasia syndrome, is essential*
525 *for osteoblast differentiation and bone development.* Cell, 1997. **89**(5): p. 765-71.
526 45. Hesse, E., et al., *Zfp521 controls bone mass by HDAC3-dependent attenuation of Runx2*
527 *activity.* J Cell Biol, 2010. **191**(7): p. 1271-83.
528 46. James, A.W., *Review of Signaling Pathways Governing MSC Osteogenic and Adipogenic*
529 *Differentiation.* Scientifica (Cairo), 2013. **2013**: p. 684736.

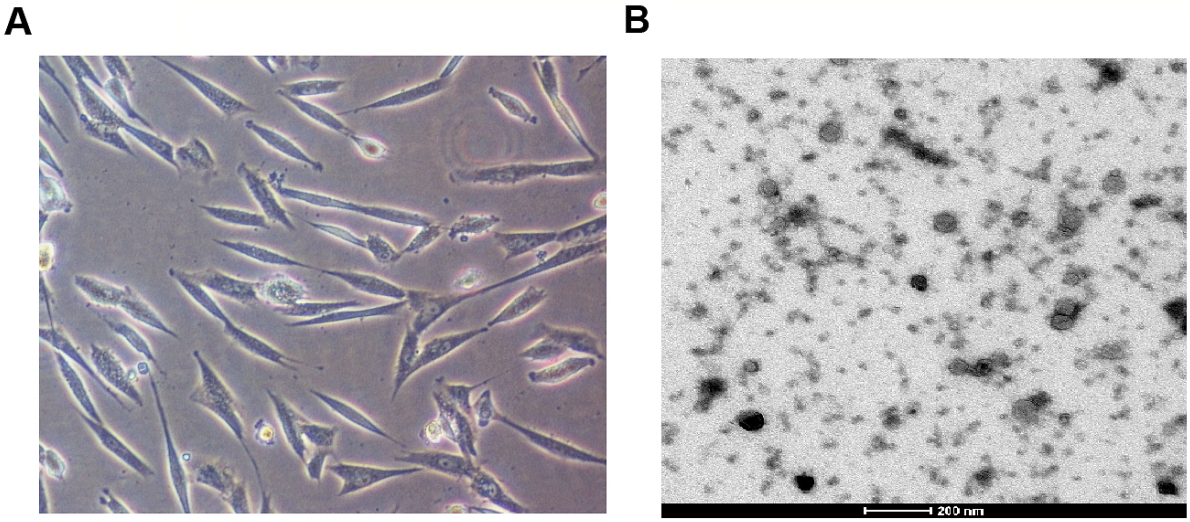

Characterization of exosomes isolated from bone marrow stem cells.
A: The primary bone marrow stem cells showed a long spindle shape.
B: Representative images of BMSC-derived exosomes observed under an electron microscope.

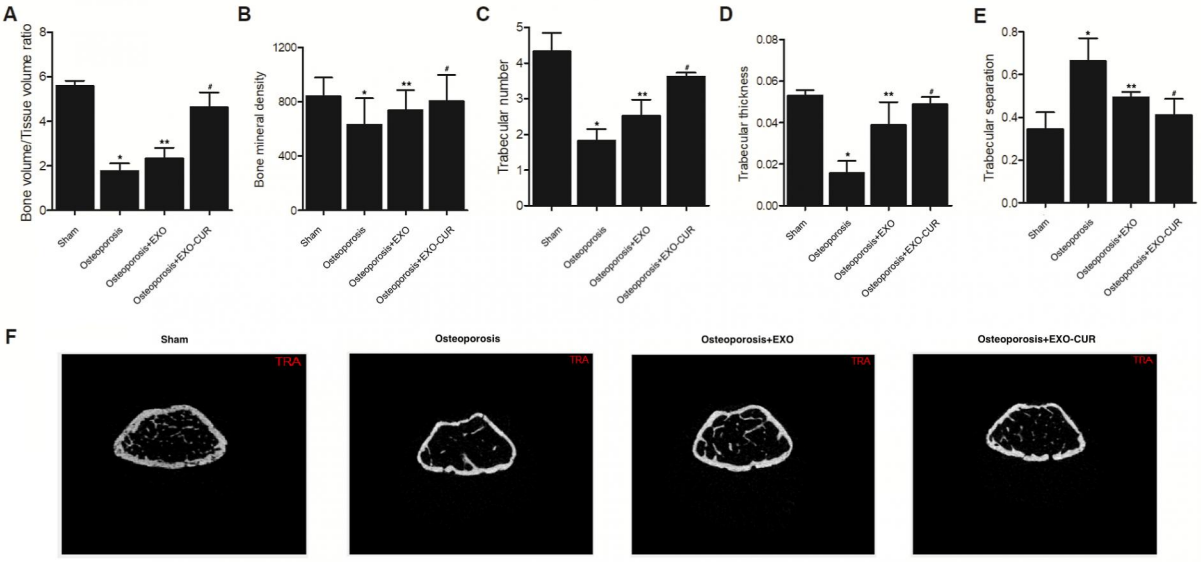

CUR treatment strengthened the therapeutic effect of BMSC-derived exosomes on osteoporosis mice (* P-value < 0.05 vs. SHAM group; ** P-value < 0.05 vs. OSTEOPOROSIS group; # P-value < 0.05 vs. OSTEOPOROSIS + CUR group).
A: CUR treatment enhanced the capability of BMSC-derived exosomes in restoring the Bone volume/Tissue volume ratio in osteoporosis mice.
B: CUR treatment enhanced the capability of BMSC-derived exosomes in restoring the Bone mineral density in osteoporosis mice.
C: CUR treatment enhanced the capability of BMSC-derived exosomes in restoring the Trabecular number in osteoporosis mice.
D: CUR treatment enhanced the capability of BMSC-derived exosomes in restoring the Trabecular thickness in osteoporosis mice.
E: CUR treatment enhanced the capability of BMSC-derived exosomes in restoring the Trabecular separation in osteoporosis mice.
F: Representative micro-CT images of mice groups.

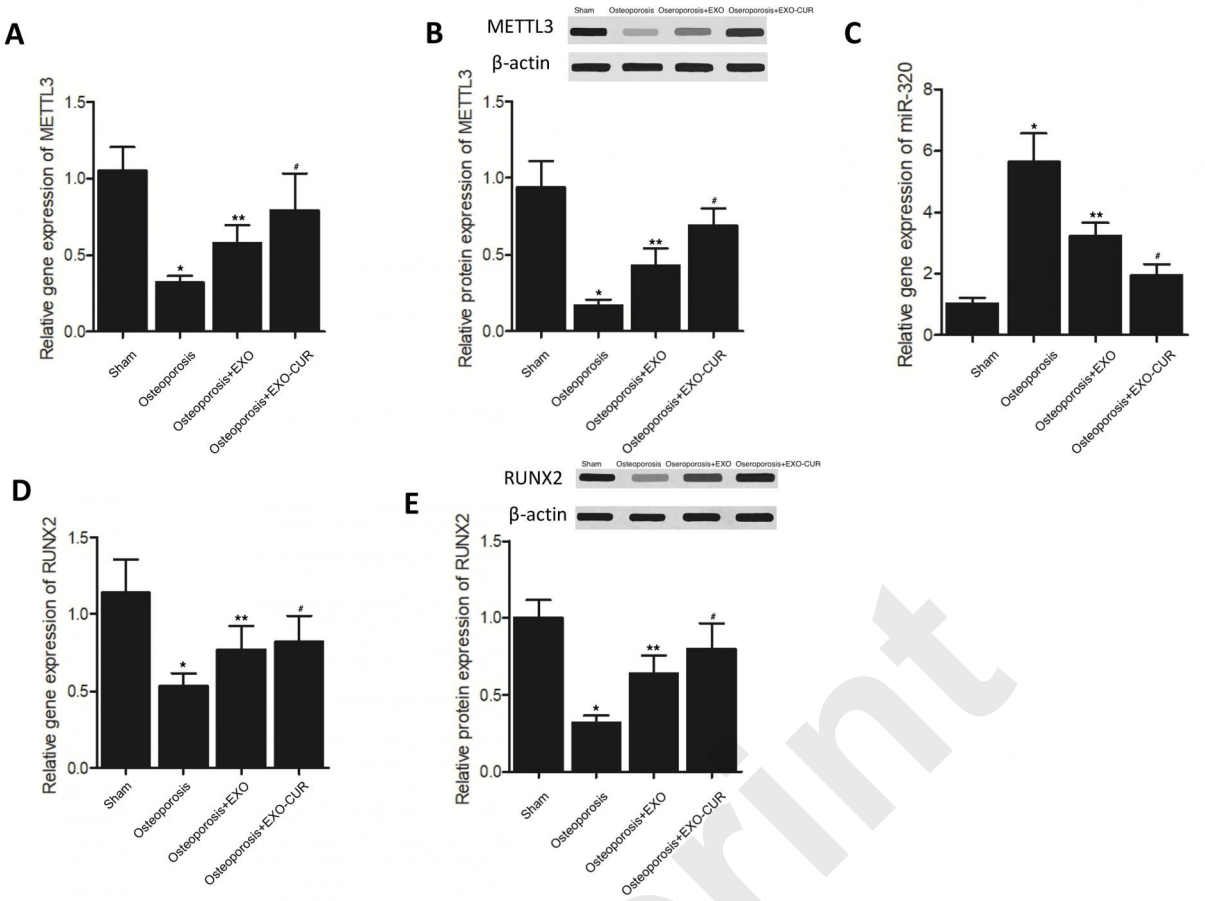

Fig.3
CUR treatment enhanced the capability of BMSC-derived exosomes in maintaining the expression of METTL3, miR-320 and RUNX2 in osteoporosis mice (* P-value < 0.05 vs. Sham group; ** P-value < 0.05 vs. Osteoporosis group; # P-value < 0.05 vs. Osteoporosis + EXO group).
A: CUR treatment enhanced the capability of BMSC-derived exosomes in maintaining the expression of METTL3 mRNA in osteoporosis mice.
B: CUR treatment enhanced the capability of BMSC-derived exosomes in maintaining the expression of METTL3 protein in osteoporosis mice.
C: CUR treatment enhanced the capability of BMSC-derived exosomes in maintaining the expression of miR-320 in osteoporosis mice.
D: CUR treatment enhanced the capability of BMSC-derived exosomes in maintaining the expression of RUNX2 mRNA in osteoporosis mice.
E: CUR treatment enhanced the capability of BMSC-derived exosomes in maintaining the expression of RUNX2 protein in osteoporosis mice.

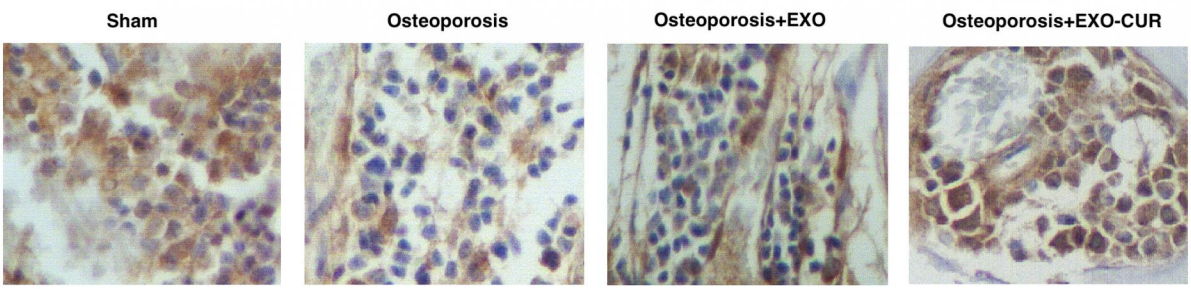

Immunohistochemistry analysis showed that CUR treatment enhanced the capability of BMSC-derived exosomes in maintaining the expression of METTL3 protein in osteoporosis mice.

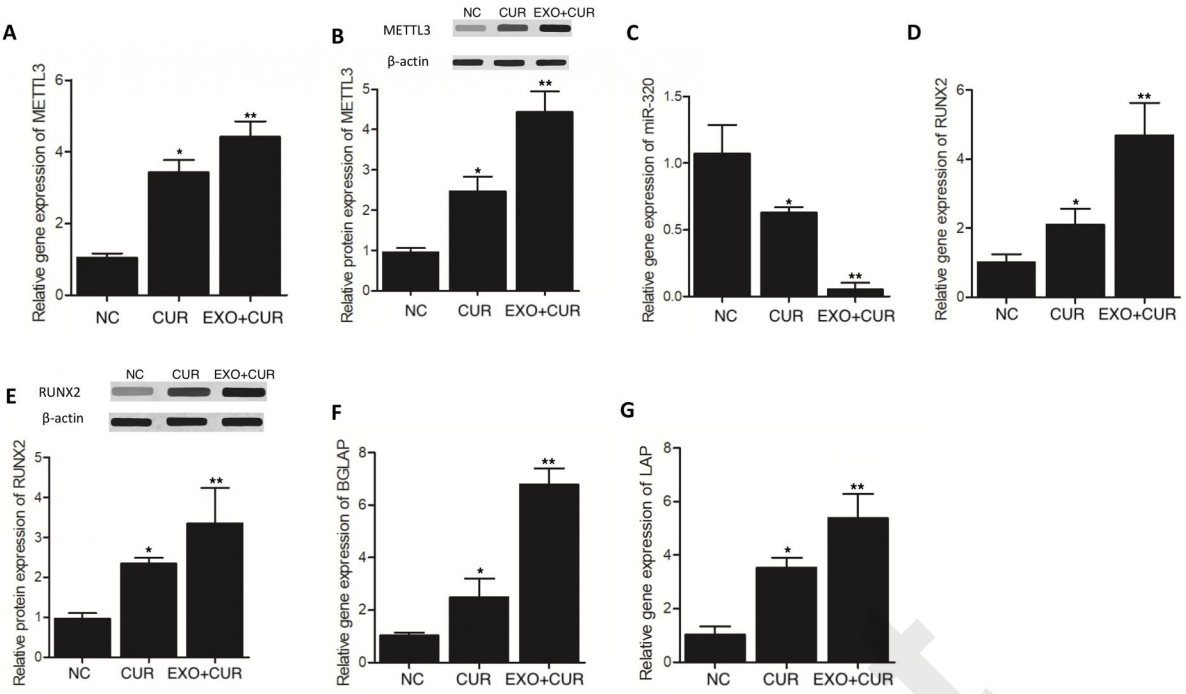

Fig.5
Exosomes derived from CUR-treated BMSCs strengthened the ability of CUR in altering the expression of METTL3, miR-320, RUNX2, BGLAP and LAP in BMSCs cells (* P-value < 0.05 vs. NC group; ** P-value < 0.05 vs. CUR group).
A: Exosomes derived from CUR-treated BMSCs strengthened the effect of CUR in promoting the expression of METTL3 mRNA in BMSCs cells.
B: Exosomes derived from CUR-treated BMSCs strengthened the effect of CUR in promoting the expression of METTL3 protein in BMSCs cells.
C: Exosomes derived from CUR-treated BMSCs strengthened the effect of CUR in suppressing the expression of miR-320 in BMSCs cells.
D: Exosomes derived from CUR-treated BMSCs strengthened the effect of CUR in promoting the expression of RUNX2 mRNA in BMSCs cells.
E: Exosomes derived from CUR-treated BMSCs strengthened the effect of CUR in promoting the expression of RUNX2 protein in BMSCs cells.
F: Exosomes derived from CUR-treated BMSCs strengthened the effect of CUR in promoting the expression of BGLAP mRNA in BMSCs cells.
G: Exosomes derived from CUR-treated BMSCs strengthened the effect of CUR in promoting the expression of LAP mRNA in BMSCs cells.

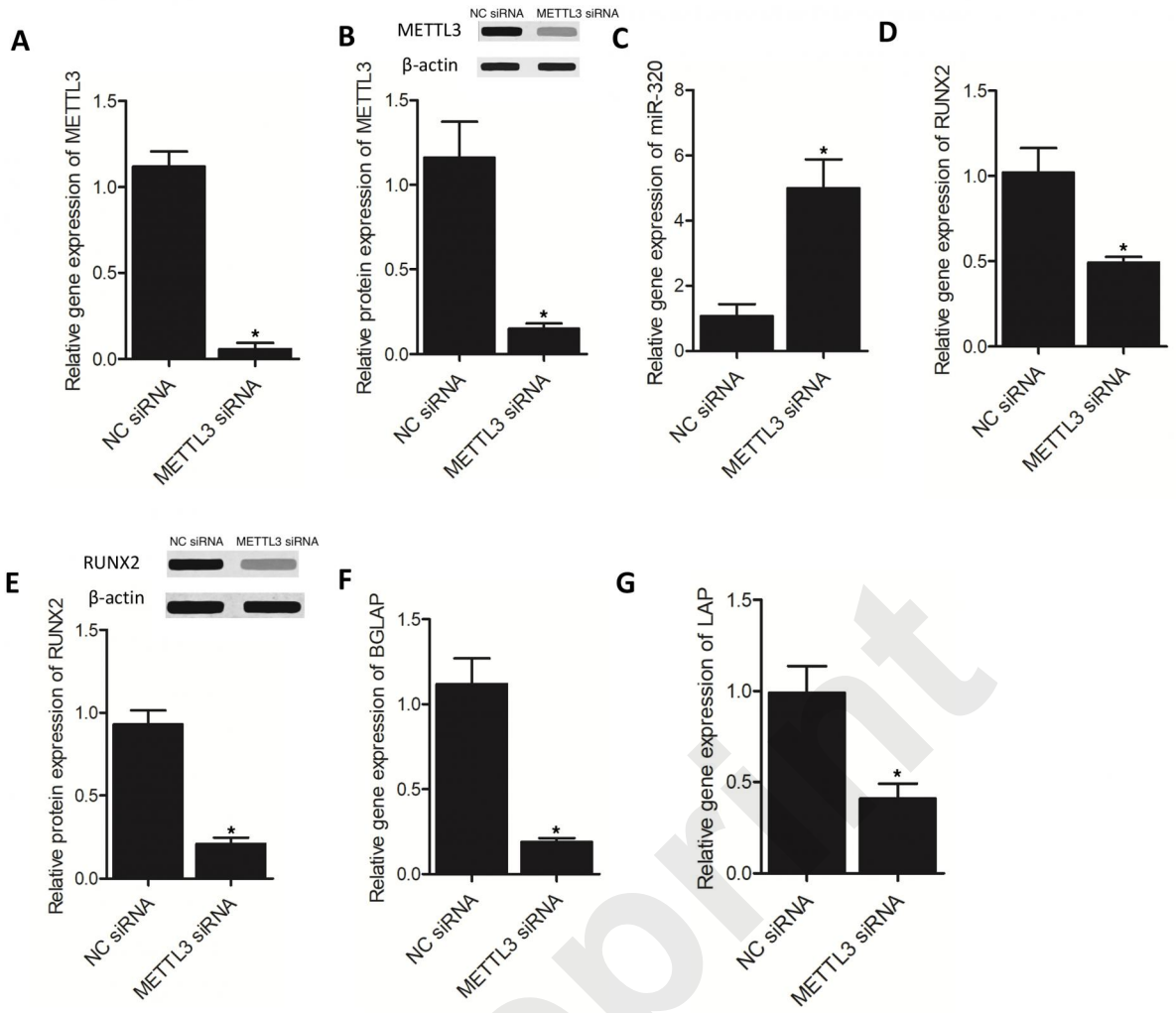

Fig.6

METTL3 siRNA transfection altered the expression of METTL3, miR-320, RUNX2, BGLAP and LAP in BMSCs cells (* P-value < 0.05 vs. NC siRNA group).

A: The expression of METTL3 mRNA was suppressed by METTL3 siRNA in BMSCs cells.

B: The expression of METTL3 protein was suppressed by METTL3 siRNA in BMSCs cells.

C: The expression of miR-320 was increased by METTL3 siRNA in BMSCs cells.

D: The expression of RUNX2 mRNA was suppressed by METTL3 siRNA in BMSCs cells.

E: The expression of RUNX2 protein was suppressed by METTL3 siRNA in BMSCs cells.

F: The expression of BGLAP mRNA was suppressed by METTL3 siRNA in BMSCs cells.

G: The expression of LAP mRNA was suppressed by METTL3 siRNA in BMSCs cells.

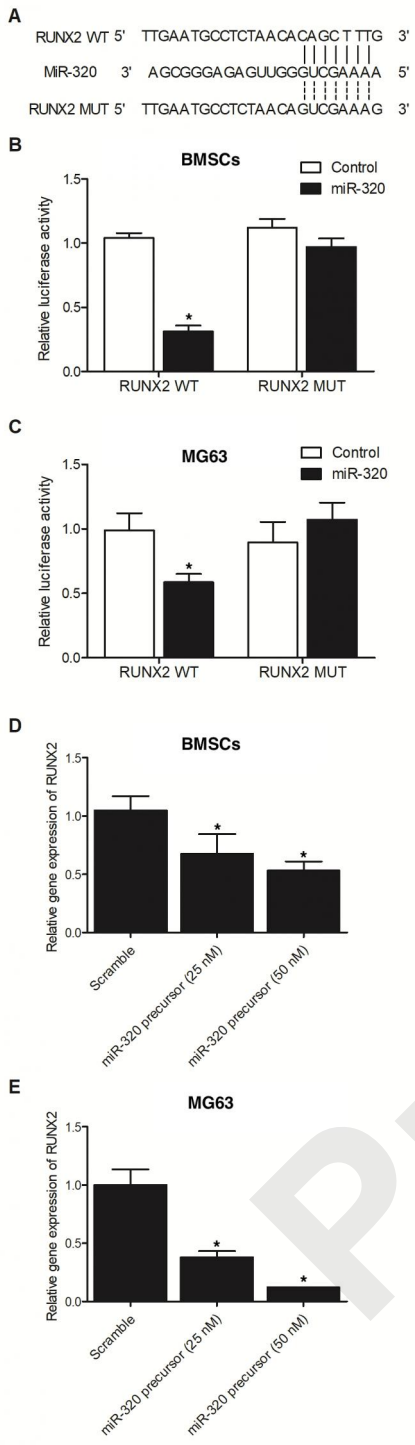

MiR-320 suppressed the expression of RUNX2 through binding to its 3' UTR.
A: Sequence analysis indicated that miR-320 could potentially bind to the 3' UTR of RUNX2.
B: The luciferase activity of wild type RUNX2 was remarkably suppressed by miR-320 in BMSCs cells (* P-value < 0.05 vs. control group).
C: The luciferase activity of wild type RUNX2 was remarkably suppressed by miR-320 in MG63 cells (* P-value < 0.05 vs. control group).
D: The expression of RUNX2 mRNA was repressed by miR-320 precursors in a dose dependent manner in BMSCs cells (* P-value < 0.05 vs. scramble group).

E: The expression of RUNX2 mRNA was repressed by miR-320 precursors in a dose dependent manner in MG63 cells (* P-value < 0.05 vs. scramble group).

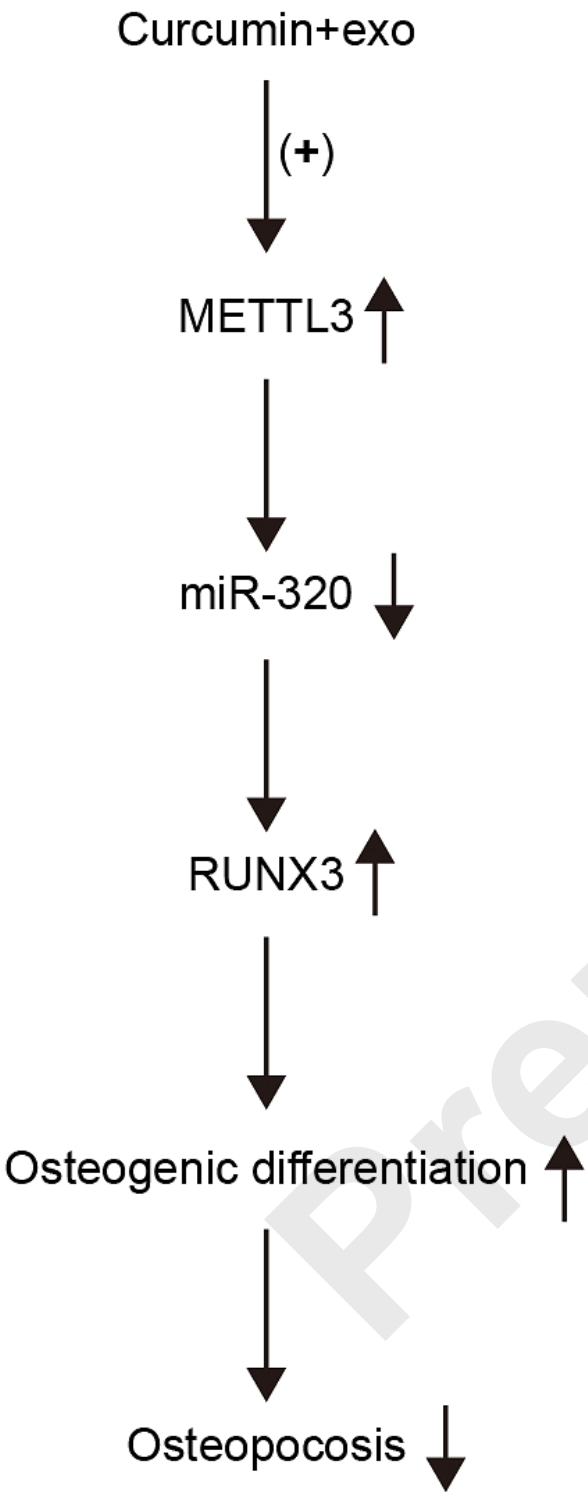

Schematic illustration of the study.